Int. J. Anal. Appl. (2026), 24:385

International Journal of Analysis and Applications

Codimension-Two Bifurcation Analysis of a Discrete-Time Predator–Prey System with Allee Effects and Environmental Factors

Abdulaziz Almaslokh[1], A. A. Elsadany[1,*], B. Alreshidi[1], A. S. Zaki[2]

[1]*Mathematics Department, College of Science and Humanities Studies in Al-Kharj, Prince Sattam bin Abdulaziz University, Al-Kharj 11942, Saudi Arabia*

[2]*Mathematics Department, Faculty of Science, Aswan University, Aswan 81528, Egypt*

[*]*Corresponding author:* aelsadany1@yahoo.com

Abstract. This paper is devoted to the codimension two bifurcation analysis of a discrete-time predator-prey model of two species, with consideration of Allee effects, prey refuge, water availability, and the effect of moonlight. We study three types of codimension-two bifurcations, 1:2, 1:3 and 1:4 resonances, in detail using bifurcation theory and numerical continuation techniques in the reduced discrete-time model. The conditions for codimension-two bifurcations are established by deriving the approximation normal form via the transformation of many parameters and variables. Our theoretical conclusions are supported by numerical simulations and the model shows complex dynamical properties such as quasi-periodic orbits and chaotic sets.

1. Introduction

One of the important frameworks of biological dynamics is predator-prey model by Lotka and Volterra showing the predator-prey oscillations [1–7]. Holling [3] introduced three types of functional response—Type I, II, and III—to better describe predator behaviour at different prey concentrations, although they were simple. Discrete-time models, especially for species with non-overlapping generations, display a broader spectrum of dynamic behaviors, including chaos, flip bifurcations, heteroclinic cycles, and Neimark-Sacker bifurcations, as pointed out by researchers [8–13]. Predators can not only prey on prey but also disrupt prey's physiology and behavior. Therefore, the prey species can have different anti-predator strategies including harvesting adaptation, use of refuge and behavioural change due to fear, which play an important role in predator-prey dynamics [14–16]. The center manifold theory has been used by many scholars

Received: Aug. 18, 2026.

2020 *Mathematics Subject Classification.* 39A28; 39A30; 92D25.

Key words and phrases. discrete predator–prey system; stability; codimension-two bifurcation; 1:2 resonance; 1:3 resonance; 1:4 resonance.

https://doi.org/10.28924/2291-8639-24-2026-385
ISSN: 2291-8639

© 2026 the author(s).

to study codimension-one bifurcations in discrete-time models. This is done in recent years . Instances of this kind of bifurcations are Neimark-Sacker and Flip. There has been an increasing interest in the examination of codimension-two bifurcation in discrete-time predator-prey systems [17–20]. Theoretical frameworks often inadequately capture the complex dynamics, even in ostensibly simple systems. Thus, numerical methods have proven valuable not only in validating analytical results but also in providing deeper insights into system dynamics.

Recently, Elsadany et al. [21] formulated a discrete-time version of the continuous predator-prey model proposed by Ashraf [22], employing the piecewise constant arguments methodology. The discrete system formulated by Elsadany et al. [21] is expressed as follows:

$$\begin{aligned} x(n+1) &= x(n)exp\Big[r(1-\frac{x(n)}{k})(\frac{x(n)}{x(n)+A}) - \frac{y(n)(a(1-\beta)+\alpha\omega)}{1+x(n)(1-\beta+qm)}\Big], \\ y(n+1) &= y(n)exp\Big[\frac{\eta x(n)(a(1-\beta)+\alpha\omega)}{1+x(n)(1-\beta+qm)} - \mu\Big]. \end{aligned} \tag{1.1}$$

The bifurcation of equilibria gives rise to the complex dynamics of an ecosystem. In [21] the authors studied codimension one bifurcation phenomena of the model by using center manifold theory to investigate flip and Neimark-Sacker bifurcations. This work presents a mathematical analysis of the complex dynamics and higher-order bifurcations of the model (1.1). We will study in detail the codimension-two bifurcations of resonance phenomena and draw the complicated patterns associated with the different types of bifurcations by computing the normal forms. We study codimension-two bifurcations by an effective analytical method widely used in the theory of discrete-time models [23–27]. We compute the normal form coefficients to prove the non-degeneracy of these bifurcations in the model, which is a necessary condition to validate the existence of these bifurcations. The literature on codimension-one bifurcations and chaotic dynamics in continuous and discrete systems is extensive, but analyzes of codimension-two bifurcations are relatively sparse [28–32].

In this paper, the present challenges and the prior work are considered to analyze the codimension-two bifurcations in the suggested discrete predator-prey model. We present the 1:2, 1:3 and 1:4 resonance bifurcations of the system. We plot the curves in the original variables and parameters. Numerical simulations validate our theoretical predictions and reveal a wide variety of dynamical behaviors, from quasi-periodic orbits to chaotic sets. The structure of the paper is as follows. The discussion of the codimension-two bifurcations is presented in Section 2. In section 3 we introduce the numerical continuation to verify the analytical conclusions of the codimension bifurcations. We end with a quick summary of our mathematical remarks in Section 4.

2. Codimension-Two Bifurcation Analysis

This section discusses the presence codimension-two bifurcation analysis around the positive interior equilibrium points in system (1.1). The model (1.1) has three non-negative equilibrium

points, as indicated below:

(1) The trivial fixed point $E_0 = (0, 0)$;
(2) The semi-trivial fixed point $E_1 = (k, 0)$;
(3) The interior fixed point $E_2 = (x^*, y^*) = (\frac{\mu}{(1-\beta)(a\eta-\mu)+\eta\alpha\omega-\mu qm}, \frac{rx^*(k-x^*)(1+x^*(1-\beta+qm))}{k(x^*+A)(a-a\beta+\alpha\omega)})$.

The study of the probable bifurcation scenarios in codimension one is conducted by utilizing normal forms and the important nondegeneracy coefficients at E_0, E_1 and E_2 of model (1.1). There are the results for stability and bifurcations along the center manifold that take place in codimension one that are presented in [21]. As mentioned in references ([23–27]), we will explore the fascinating strong resonance phenomena at the positive fixed point $E_2(x^*, y^*)$ for the model (1.1) in this section. The Jacobian matrix evaluated at $E_2(x^*, y^*)$ is expressed as

$$J(x, y) = \begin{pmatrix} 1 + x^*\left[\frac{r(Ak-x^{*2}-2Ax^*)}{k(x^*+A)^2} + \frac{y^*(a-a\beta+\alpha\omega)(1-\beta+qm)}{(1+x^*(1-\beta+qm))^2}\right] & -\frac{x^*(a-a\beta+\alpha\omega)}{1+x^*(1-\beta+qm)} \\ \frac{\eta y^*(a-a\beta+\alpha\omega)}{(1+x^*(1-\beta+qm))^2} & 1 \end{pmatrix}.$$

The characteristic equation at this stationary point, which is known as point E_2, can be stated as follows:

$$\lambda^2 + p(x^*, y^*)\lambda + q(x^*, y^*) = 0, \tag{2.1}$$

where

$$\begin{cases} p(x^*, y^*) = -2 - G,\ q(x^*, y^*) = 1 + G + H, \\ G = x^*\left[\frac{r(Ak-x^{*2}-2Ax^*)}{k(x^*+A)^2} + \frac{y^*(a-a\beta+\alpha\omega)(1-\beta+qm)}{(1+x^*(1-\beta+qm))^2}\right], \\ H = \frac{\eta x^* y^*(a-a\beta+\alpha\omega)^2}{(1+x^*(1-\beta+qm))^3}. \end{cases}$$

When the values of $p(x^*, y^*)$ and $q(x^*, y^*)$ are such that $p(x^*, y^*) = 2$ and $q(x^*, y^*) = 1$, the eigenvalues λ_1 and λ_2 coincide, both equaling -1. This signifies that model (1.1) exhibits a 1:2 resonance. Furthermore, if $p(x^*, y^*) = q(x^*, y^*) = 1$, then $\lambda_{1,2} = \frac{-1\pm i\sqrt{3}}{2}$. This indicates that model (1.1) demonstrates a 1:3 resonance. If $p(x^*, y^*) = 0$ and $q(x^*, y^*) = 1$, then $\lambda_{1,2} = \pm i$ is a sufficient condition. This finding suggests that model (1.1) reveals an attractive 1:4 resonance. The subsequent sets, F_{1j}, are defined as follows and effectively characterize these significant resonance phenomena:

$$F_{1j} := \{(r, A, k, a, \beta, \alpha, \omega, m, q, \eta, \mu) \in \mathbb{R}^{11}_+, p(x^*, y^*) = 4 - j, q(x^*, y^*) = 1\}, j = 2, 3, 4.$$

2.1. **The 1:2 strong resonance of model (1.1) at the Positive Fixed Point $E_2(x^*, y^*)$.** This subsection examines the circumstances under which a 1:2 resonance occurs at the Positive Fixed Point $E_2(x^*, y^*)$, utilizing bifurcation theory and normal form theory in accordance with the methodologies utilized in [23, 32, 33]. In order to continue, parameters $(\hat{r}, k, A, a, \beta, \alpha, \omega, q, m, \hat{\eta}, \mu) \in F_{12}$ are

randomly selected. Consequently, the following is a representation of model (1.1):

$$\begin{aligned} x(n+1) &= x(n)exp\Big[\hat{r}(1-\frac{x(n)}{k})(\frac{x(n)}{x(n)+A}) - \frac{y(n)(a(1-\beta)+\alpha\omega)}{1+x(n)(1-\beta+qm)}\Big], \\ y(n+1) &= y(n)exp\Big[\frac{\hat{\eta}x(n)(a(1-\beta)+\alpha\omega)}{1+x(n)(1-\beta+qm)} - \mu\Big]. \end{aligned} \tag{2.2}$$

The model (2.2) exhibits two eigenvalues, $\lambda_1 = \lambda_2 = -1$, at the fixed point E_2. To investigate the influence of the bifurcation parameters $\hat{r}$ and $\hat{\eta}$, we shall apply a little perturbation to model (2.2). This disturbance enhances our comprehension of the system's dynamics. The revised model can be articulated as follows:

$$\begin{aligned} x(n+1) &= x(n)exp\Big[(\hat{r}+\bar{r})(1-\frac{x(n)}{k})(\frac{x(n)}{x(n)+A}) - \frac{y(n)(a(1-\beta)+\alpha\omega)}{1+x(n)(1-\beta+qm)}\Big], \\ y(n+1) &= y(n)exp\Big[\frac{(\hat{\eta}+\bar{\eta})x(n)(a(1-\beta)+\alpha\omega)}{1+x(n)(1-\beta+qm)} - \mu\Big], \end{aligned} \tag{2.3}$$

where $|\bar{r}|$ and $|\bar{\eta}|$ are small perturbation parameters. Let us define $\hat{u}(n) = x(n) - x^*$ and $\hat{v}(n) = y(n) - y^*$. We can express r as $\hat{r} + \bar{r}$ and η as $\hat{\eta} + \bar{\eta}$. By using a coordinate transformation to modify the fixed point E_2 at the origin, we simplify our methodology and improve our understanding of model (2.3). This strategic shift results in a more succinct expression:

$$\begin{aligned} \hat{u}(n+1) &= a_1\hat{u}(n) + a_2\hat{v}(n) + a_{11}\hat{u}^2(n) + a_{12}\hat{u}(n)\hat{v}(n) + a_{22}\hat{v}^2(n) + O((|\hat{u}(n)| + |\hat{v}(n)|)^3), \\ \hat{v}(n+1) &= b_1\hat{u}(n) + b_2\hat{v}(n) + b_{11}\hat{u}^2(n) + b_{12}\hat{u}(n)\hat{v}(n) + b_{22}\hat{v}^2(n) + O((|\hat{u}(n)| + |\hat{v}(n)|)^3), \end{aligned} \tag{2.4}$$

both a_1, a_2, b_1, and b_2 are referenced in Appendix. Likewise, $a_{11}, a_{12}, a_{22}, b_{11}$, and b_{12} are specified in Appendix.

Let T_1 be an invertible matrix defined by

$$T_1 = \begin{pmatrix} \frac{-a_2}{1+a_1} & \frac{-a_2}{(1+a_1)^2} \\ 1 & 0 \end{pmatrix},$$

and use the translation

$$\begin{pmatrix} \hat{u} \\ \hat{v} \end{pmatrix} = T_1 \begin{pmatrix} \hat{x} \\ \hat{y} \end{pmatrix}.$$

Next, Map (2.4) is converted into

$$\begin{pmatrix} \hat{x} \\ \hat{y} \end{pmatrix} \mapsto \begin{pmatrix} -1 + a_{10}(r,\eta) & 1 + a_{01}(r,\eta) \\ b_{10}(r,\eta) & -1 + b_{01}(r,\eta) \end{pmatrix} \begin{pmatrix} \hat{x} \\ \hat{y} \end{pmatrix} + \begin{pmatrix} \hat{f}(\hat{x},\hat{y},r,\eta) \\ \tilde{g}(\hat{x},\hat{y},r,\eta) \end{pmatrix}, \tag{2.5}$$

where

$$\hat{f}(\hat{x},\hat{y},r,\eta) = \sum_{2\le j+k\le 3} \hat{f}_{jk}(r,\eta)\,\hat{x}^j\hat{y}^k,$$

$$\hat{g}(\hat{x},\hat{y},r,\eta) = \sum_{2\le j+k\le 3} \hat{g}_{jk}(r,\eta)\,\hat{x}^j\hat{y}^k,$$

and

$$\begin{cases} a_{10}(r,\eta) = 2 + \frac{aa_2\eta y^*(-1+\beta)}{(1+a_1)(-1+x^*(-1+\beta-qm))^2} - \frac{a_2m\alpha\eta y^*}{(1+a_1)(-1+x^*-\beta x+qmx^*)^2}, \\ \\ a_{01}(r,\eta) = -1 + \frac{a_2\eta y^*(-a-a\beta-\alpha\omega)}{(1+a_1)^2(-1+x^*(-1+\beta-qm))^2}, \\ \\ b_{10}(r,\eta) = \frac{1}{a_2k(A+x^*)^2(-1+x^*(-1+\beta-qm))^2}\Big[ak((A+x^*)^2(-1+\beta)(x^{*2}(1+a_1)^2(-1+\beta-qm) \\ \quad -x^*(1+a_1)(1+a_1+a_2y^*(1-\beta+qm)) - a_2^2\eta y^*) + A^2k\alpha(-x^{*2}(1+a_1)(-1+\beta-qm) \\ \quad +x^*(1+a_1)(1+a_1+a_2y^*(1-\beta+qm)) + a_2^2y^*\eta\omega + x^{*2}(-kx^*\alpha\omega(1+a_1)^2(-1+x^*(-1 \\ \quad +\beta-qm)) \\ \quad +a_2^2ky^*\alpha\eta\omega - a_2x^*(1+a_1)(r(1+x^*-x\beta+qmx^*)^2 + k\alpha\omega y^*(-1+\beta-qm))) \\ \quad +Ax^*(-2k\alpha\omega x^*(1+a_1)^2(-1+x^*(-1+\beta-qm)) + 2a_2^2k\alpha\eta\omega y^* + a_2(1+a_1)(-2rx^*(1 \\ \quad +x^*-x^*\beta+qmx^*)^2 \\ \quad +k(r(1+x^*-x^*\beta+qmx^*)^2 + 2\omega\alpha x^*y^*(1-\beta+qm))))\Big], \\ b_{01}(r,\eta) = 1 + \frac{1}{a_2k(A+x^*)^2(-1+x^*(-1+\beta-qm))^2}\Big[ak((A+x^*)^2(-1+\beta)(x^{*2}(1+a_1)^2(-1+\beta-qm) \\ \quad -x^*(1+a_1)(1+a_1+a_2y^*(1-\beta+qm)) - a_2^2\eta y^*) + A^2k\alpha(-x^{*2}(1+a_1)(-1+\beta-qm) \\ \quad +x^*(1+a_1)(1+a_1+a_2y^*(1-\beta+qm)) + a_2^2y^*\eta\omega + x^{*2}(-kx^*\alpha\omega(1+a_1)^2(-1+x^*(-1 \\ \quad +\beta-qm)) \\ \quad +a_2^2ky^*\alpha\eta\omega - a_2x^*(1+a_1)(r(1+x^*-x*\beta+qmx^*)^2 + k\alpha\omega y^*(-1+\beta-qm))) \\ \quad +Ax^*(-2k\alpha\omega x^*(1+a_1)^2(-1+x^*(-1+\beta-qm)) + 2a_2^2k\alpha\eta\omega y^* \\ \quad +a_2(1+a_1)(-2rx^*(1+x^*-x^*\beta+qmx^*)^2 + k(r(1+x^*-x^*\beta+qmx^*)^2 + 2\omega\alpha x^*y^*(1-\beta \\ \quad +qm))))\Big], \end{cases}$$

$$\begin{cases} \hat{f}_{20}(r,\eta) = \frac{a_2^2\eta y(1-\beta+qm)(a(-1+\beta)-\alpha\omega)(-2+2x^*(-1+\beta-qm)+a\eta(-1+\beta)-\alpha\eta\omega))}{(1+a_1)^2(1+x^*-x^*\beta+qmx^*)^4}, \\ \\ \hat{f}_{11}(r,\eta) = \frac{2a_2^2\eta y^*(-1+\beta-qm)(a(-1+\beta)-\alpha\omega)(-2+2x^*(-1+\beta-qm)+a\eta(-1+\beta)-\alpha\eta\omega))}{(1+a_1)^3(1+x^*-x^*\beta+qmx^*)^4}, \\ \\ \hat{f}_{02}(r,\eta) = \frac{2a_2^2\eta y^*(-1+\beta-qm)(a(-1+\beta)-\alpha\omega)(-2+2x(-1+\beta-qm)+a\eta(-1+\beta)-\alpha\eta\omega))}{(1+a_1)^4(1+x^*-x^*\beta+qmx^*)^4}, \\ \\ \hat{f}_{30}(r,\eta) = \hat{f}_{12}(r,\eta) = \hat{f}_{21}(r,\eta) = \hat{f}_{03}(r,\eta) = 0, \end{cases}$$

$$
\begin{cases}
\hat{g}_{20}(r,\eta) = -\frac{A^2a_2r(Ak(k-4x^*)+x^*(k^2(1+r)-4kx^*(1-r)+4rx^{*2}))}{k^2(A+x^*)^4} - \frac{y^*(1+a_1)^2(a-a\beta+\alpha\omega)^2}{a_2((1+x^*-x\beta+qmx^*)^4)} \\
\quad -\frac{a_2^2\eta y^*(a(-1+\beta)-\alpha\omega)(-2+2x^*(-1+\beta-qm)+a\eta(-1+\beta)-\alpha\eta\omega))}{(1+a_1)(1+x^*-x\beta+qmx^*)^4} \\
\quad -\frac{1}{k(A+x^*)^2(-1+x^*(-1+\beta-qm))^3}\Big[(1+a_1)(a(-1+\beta)-\alpha\omega)(A^2k(1+x^*(-1+\beta-qm)(-1 \\
\quad +ay^*(-1+\beta)-y^*\alpha\omega)) \\
\quad +2Akx^*(1+x^*(-1+\beta-qm)(-1+ay^*(-1+\beta)-y^*\alpha\omega))+x^{*2}(-rx^*(1+x^*-x^*\beta \\
\quad +qmx^*)^2 \\
\quad +k(1+x^*(-1+\beta-qm)(-1+ay^*(-1+\beta)-y^*\alpha\omega))))\Big],
\end{cases}
$$

$$
\begin{cases}
\hat{g}_{11}(r,\eta) = \frac{1}{(1+a_1)^3}\Big[\frac{2ra_2A^2(1+a_1)^2(Ak(k-4x^*)+x^*(k^2(1+r)-4kx^*(1+r)+4rx^{*2}))}{k^2(A+x^*)^4} \\
\quad +\frac{1}{Ar(A+x^*)^4}\Big(\frac{4a_2rx^{*2}+8ra_1a_2x^{*3}+4ra^2{}_1a_2x^{*3}}{k} \\
\quad -\frac{8ra_2x^{*4}+16ra_1a_2x^{*4}}{k^2} - \frac{8ra^2{}_1a_2x^{*4}}{k^2} + 2a_2x^*(A+x^*) + 4a_1a_2x^*(A+x^*) + 2a^2{}_1a_2x^*(A+x^*) \\
\quad -2a_2(A+x^*)^2 \\
\quad -4a_1a_2(A+x^*)^2 - 2a_1^2a_2(A+x^*)^2 + \frac{4a_2x^*(A+x^*)^2+8a_1a_2x^*(A+x^*)^2+2a_1^2a_2(A+x^*)^2}{k} \\
\quad -\frac{4aa_2x^*y^*(A+x^*)^2}{(1-x^*-x^*\beta+qmx^*)^2} \\
\quad -\frac{8aa_1a_2x^*y^*(A+x^*)^2}{(1-x^*-x^*\beta+qmx^*)^2} + \frac{4aa_1^2a_2x^*y^*(A+x^*)^2}{(1+x^*-x^*\beta+qmx^*)^2} + \frac{8aa_2x^{*2}y^*(A+x^*)^2}{(1+x^*-x^*\beta+qmx^*)^2} + \frac{16aa_1a_2x^{*2}y^*(A+x^*)^2}{(1+x^*-x^*\beta+qmx^*)^2}\Big)\Big],
\end{cases}
$$

$$
\begin{cases}
\hat{g}_{02}(r,\eta) = \frac{a_2}{(1+a_1)^3}\Big[\frac{-r^2x^{*5}(1+a_1)}{k^2(A+x^*)^4} - \frac{A^2r(1+a_1)(Ak(k-4x^*)+x^*(k^2(1+r)-4kx^*(1+r)+4rx^{*2}))}{k^2(A+x^*)^4} \\
\quad -\frac{1}{y^*(1+x^*-x^*\beta+qmx^*)^4(-1-\beta-qm)(a(-1+\beta)-\alpha\omega)}\Big(2-2a_2\eta-aa_2\eta^2+aa_2\beta\eta^2 \\
\quad -a_2\alpha\omega\eta^2+x^*(-1+\beta-qm)(-2+ay^*(-1+\beta)+2a_2\eta-y^*\alpha\omega) \\
\quad +a_1(2+x^*(-1+\beta-qm)(-2+ay^*(-1+\beta)-\alpha\omega y^*))\Big) \\
\quad +\Big(rx^{*2}(1+a_1)(2x^*(1+x^{*2}(1-\beta+qm)^2+x^*(-1+\beta-qm)(-2+ay^*(-1+\beta) \\
\quad -y^*\alpha\omega)) \\
\quad +A(1+x^{*2}(1-\beta+qm)^2+2x^*(1-\beta+qm)(-1+ay^*(-1+\beta)-\alpha\omega y^*)\Big)\Big], \\
\hat{g}_{30}(r,\eta) = \hat{g}_{12}(r,\eta) = \hat{g}_{21}(r,\eta) = \hat{g}_{03}(r,\eta) = 0.
\end{cases}
$$

We now utilize a nonsingular linear coordinate transformation, defined by

$$
\begin{pmatrix} \hat{x} \\ \hat{y} \end{pmatrix} = \begin{pmatrix} 1+a_{01}(r,\eta) & 0 \\ -a_{10}(r,\eta) & 1 \end{pmatrix} \begin{pmatrix} \tilde{x} \\ \tilde{y} \end{pmatrix}.
$$

Therefore, Equation (2.5) has been effectively transformed into

$$
\begin{pmatrix} \tilde{x} \\ \tilde{y} \end{pmatrix} \mapsto \begin{pmatrix} -1 & 1 \\ \theta_1(r,\eta) & -1+\theta_2(r,\eta) \end{pmatrix} \begin{pmatrix} \tilde{x} \\ \tilde{y} \end{pmatrix} + \begin{pmatrix} \tilde{f}(\tilde{x},\tilde{y},r,\eta) \\ \tilde{g}(\tilde{x},\tilde{y},r,\eta) \end{pmatrix}, \tag{2.6}
$$

where

$$\tilde{f}(\tilde{x},\tilde{y},r,\eta)=\sum_{2\leq j+k\leq 3}\tilde{f}_{jk}(r,\eta)\tilde{x}^j\tilde{y}^k,$$
$$\tilde{g}(\tilde{x},\tilde{y},r,\eta)=\sum_{2\leq j+k\leq 3}\tilde{g}_{jk}(r,\eta)\tilde{x}^j\tilde{y}^k,$$

and

$$\begin{cases}\theta_1(r,\eta)=-a_{10}b_{01}+b_{10}+a_{01}b_{10},\\ \theta_2(r,\eta)=a_{10}+b_{01},\\ \tilde{f}_{20}(r,\eta)=\frac{1}{1+a_{01}}[a_{02}a_{10}^2+(1+a_{01})(-a_{10}a_{11}+a_{20}+a_{01}a_{20})],\\ \tilde{f}_{11}(r,\eta)=\frac{-2a_{02}a_{10}+a_{11}+a_{01}a_{11}}{1+a_{01}},\ \tilde{f}_{02}(r,\eta)=\frac{a_{02}}{1+a_{01}},\\ \tilde{f}_{30}(r,\eta)=\tilde{f}_{12}=\tilde{f}_{21}=\tilde{f}_{03}=0,\\ \tilde{g}_{20}(r,\eta)=\frac{a_{02}a_{10}^3+(1+a_{01})\Big(a_{10}^2(-a_{11}+b_{02})+a_{10}(1+a_{01})(a_{20}-b_{11})+b_{20}(1+a_{01})^2\Big)}{1+a_{01}},\\ \tilde{g}_{11}(\delta,r)=\frac{-2a_{02}a_{10}^2+(1+a_{01})(a_{10}a_{11}-2a_{10}b_{02}+b_{11}+a_{01}b_{11})}{1+a_{01}},\\ \tilde{g}_{02}(r,\eta)=b_{02}+\frac{a_{02}a_{10}}{1+a_{01}},\\ \tilde{g}_{30}(r,\eta)=\tilde{g}_{12}(r,\eta)=\tilde{g}_{21}(r,\eta)=\tilde{g}_{03}(r,\eta)=0.\end{cases}$$

Consequently, we do the subsequent transformation:

$$\begin{aligned}\tilde{x}&=\xi+\sum_{2\leq j+k\leq 3}\Phi_{jk}(\hat{r},\hat{\eta})\xi^j\zeta^k,\\ \tilde{y}&=\chi+\sum_{2\leq j+k\leq 3}\Psi_{jk}(\hat{r},\hat{\eta})\xi^j\zeta^k.\end{aligned}\tag{2.7}$$

The coefficients Φ_{jk} and ψ_{jk} are ascertained by the subsequent relationships:

$$\begin{cases}\Phi_{20}=\frac{1}{2}\tilde{f}_{20}+\frac{1}{4}\tilde{g}_{20},\ \Phi_{11}=\frac{1}{2}\tilde{f}_{20}+\frac{1}{2}\tilde{f}_{11}+\frac{1}{2}\tilde{g}_{20}+\frac{1}{4}\tilde{g}_{11},\\ \Phi_{02}=\frac{1}{4}\tilde{f}_{11}+\frac{1}{2}\tilde{f}_{02}+\frac{1}{8}\tilde{g}_{20}+\frac{1}{4}\tilde{g}_{11}+\frac{1}{4}\tilde{g}_{02},\\ \Psi_{20}=\frac{1}{2}\tilde{g}_{20},\ \Psi_{11}=\frac{1}{2}\tilde{g}_{20}+\frac{1}{2}\tilde{g}_{11},\ \Psi_{02}=\frac{1}{4}\tilde{g}_{11}+\frac{1}{2}\tilde{g}_{02}.\end{cases}$$

By employing transformation (2.7) and its inverse, the resultant equation can be derived as follows:

$$\begin{pmatrix}\xi\\ \chi\end{pmatrix}\mapsto\begin{pmatrix}-1 & 1\\ \theta_1(r,\eta) & 1+\theta_2(r,\eta)\end{pmatrix}\begin{pmatrix}\xi\\ \chi\end{pmatrix}+\begin{pmatrix}\Gamma(\tilde{x},\tilde{y},r,\eta)\\ \Sigma(\tilde{x},\tilde{y},r,\eta)\end{pmatrix},\tag{2.8}$$

where

$$\Gamma(\tilde{x},\tilde{y},r,\eta)=\xi+\sum_{2\leq j+k\leq 3}\gamma_{jk}(r,\eta)\xi^j\chi^k+O\Big((|\xi|,|\chi|)^4\Big),$$
$$\Sigma(\tilde{x},\tilde{y},r,\eta)=\chi+\sum_{2\leq j+k\leq 3}\sigma_{jk}(r,\eta)\xi^j\chi^k+O\Big((|\xi|,|\chi|)^4\Big),$$

where γ_{jk} and σ_{jk} are defined as follows:

$$\begin{cases} \gamma_{20}(r,\eta) = \tilde{f_{20}} + \psi_{20} - 2\phi_{20} - \phi_{02}\theta_1^2 + \phi_{11}\theta_1, \\ \gamma_{11}(r,\eta) = \tilde{f_{11}} + \psi_{11} - 2\phi_{02}\theta_1(1+\theta_2) + \phi_{11}(\theta_2 - \theta_1) + 2\phi_{20}, \\ \gamma_{02}(r,\eta) = \tilde{f_{02}} + \psi_{02} - \phi_{02}(1 + (1+\theta_2)^2) + \phi_{11}(\theta_2 + 1) - \phi_{20}, \\ \sigma_{20}(r,\eta) = \tilde{g_{20}} - \psi_{02}\theta_1^2 + \psi_{11}\theta_1 + \psi_{20}\theta_2 + \psi_{20}\theta_1, \\ \sigma_{11}(r,\eta) = \tilde{g_{11}} - 2\psi_{02}\theta_1(\theta_2+1) + \psi_{11}(2 - \theta_1 + 2\theta_2) + 2\psi_{20} + \phi_{11}\theta_1, \\ \sigma_{02}(r,\eta) = \tilde{g_{02}} - \psi_{02}\theta_2(1+\theta_2) - \psi_{11}(1+\theta_2) - \psi_{20} + \phi_{02}\theta_1. \end{cases}$$

By designating $\gamma_{jk} = \sigma_{jk} = 0$ for instances where $j+k$ equals 2, all quadratic terms are completely eradicated. Additionally, establishing $\gamma_{jk} = \sigma_{jk} = 0$ for $j+k=3$ eliminates all cubic terms except for the resonant ones. For $j+k=3$, this condition results in a system including Φ_{jk} and Ψ_{jk}, from which their values can be ascertained. Through these changes, Map (2.6) is transformed into the 1:2 resonance normal form as follows:

$$\begin{pmatrix} \xi \\ \chi \end{pmatrix} \mapsto \begin{pmatrix} -\xi + \chi \\ \theta_1(r,\eta)\xi + (-1 + \theta_2(r,\eta))\chi + C(r,\eta)\xi^3 + D(r,\eta)\xi^2\chi \end{pmatrix} + O\Big((|\xi| + |\chi|)^4\Big), \tag{2.9}$$

when $C(r,\eta) = \sigma_{30}$ and $D(r,\eta) = \sigma_{21}$, and specifically for the case where $(r,\eta) = (\hat{r},\hat{\eta})$, the functions $\theta_1(r,\eta)$ and $\theta_2(r,\eta)$ both evaluate to 0.

$$C(\hat{r},\hat{\eta}) = \tilde{g}_{30} + \tilde{f_{20}}\tilde{g}_{20} + \tfrac{1}{2}\tilde{g}_{20}^2 + \tfrac{1}{2}\tilde{g}_{20}\tilde{g}_{11},$$
$$D(\hat{r},\hat{\eta}) = \tilde{g}_{21} + 3\tilde{f_{30}} + \tfrac{1}{2}\tilde{f_{20}}\tilde{g}_{11} + \tfrac{5}{4}\tilde{g}_{20}\tilde{g}_{11} + \tilde{g}_{20}\tilde{g}_{02} + 3\tilde{f_{20}} + \tfrac{5}{2}\hat{f_{20}}\hat{g}_{20} + \tfrac{5}{2}\tilde{f_{11}}\tilde{g}_{20} + \tilde{g}_{20}^2 + \tfrac{1}{2}\tilde{g}_{11}^2$$

The following significant theorem can be effectively demonstrated by employing Theorem 9.3 and Lemma 9.10 from the reference [23].

Theorem 2.1. *Letting $C(\hat{r},\hat{\eta}) \neq 0$ is non-zero and the expression $D(\hat{r},\hat{\eta}) + 3C(\hat{r},\hat{\eta})$ is also non-zero, then it follows that Map (1.1) will exhibit specific and significant dynamical behaviors:*

(1) *The existence of a significant fixed point for $\theta_1 < 0$ is indicated by the presence of a flip bifurcation curve at $F = \{(\theta_1,\theta_2) : \theta_1 = 0\}$. This establishes a critical threshold in the system's dynamics that should not be overlooked;*

(2) *A unique and non-degenerate Neimark–Sacker bifurcation curve is readily obvious:*

$$H = \{(\theta_1,\theta_2) : \theta_1 = -\theta_2 + O((|\theta_1| + |\theta_2|)^2), \theta_1 < 0\};$$

(3) *A bifurcation curve that is heteroclinic is present:*

$$HL = \{(\theta_1,\theta_2) : \theta_1 = -\frac{5}{3}\theta_2 + O\Big((|\theta_1| + |\theta_2|)^2\Big), \theta_1 < 0\}.$$

Remark 2.1. *The model (1.1) is highly sensitive to bifurcation parameters, as shown by a strong 1:2 resonance, which greatly affects its complex dynamics. The non-degenerate Neimark-Sacker bifurcation is biologically significant as it creates periodic or quasi-periodic population-resource oscillations when the parameters (r,η) are modified within the area $(\hat{r},\hat{\eta})$. Constant oscillations, population shifts, and system chaos can result from these changes. These dynamics result from cycles every 2, 4, or 8 units of time or from homoclinic structures.*

2.2. **A strong resonance of 1:3 at the Positive Fixed Point of model (1.1)** $E_2(x^*, y^*)$**.** At the critical point $E_2(x^*, y^*)$, this part shows that model (1.1) has a 1:3 strong resonance bifurcation. Our bifurcation parameters are r and η, and we assume that the set of parameters $(\tilde{r}, k, A, a, \beta, \alpha, \omega, q, m, \tilde{\eta}, \mu)$ is part of F_{1j}. Model (1.1) changes into

$$\begin{aligned} x(n+1) &= x(n)exp\Big[\tilde{r}(1-\frac{x(n)}{k})(\frac{x(n)}{x(n)+A}) - \frac{y(n)(a(1-\beta)+\alpha\omega)}{1+x(n)(1-\beta+qm)}\Big], \\ y(n+1) &= y(n)exp\Big[\frac{\tilde{\eta}x(n)(a(1-\beta)+\alpha\omega)}{1+x(n)(1-\beta+qm)} - \mu\Big]. \end{aligned} \tag{2.10}$$

When the model (2.10) is evaluated at the positive fixed point E_2, it shows two eigenvalues, which are written as $\lambda_{1,2} = \frac{-1\pm i\sqrt{3}}{2}$. The variables $\tilde{u}(n) = x(n) - x^*$ and $\tilde{v}(n) = y(n) - y^*$ are now known. The model (2.10) changes into this shape.

$$\begin{aligned} \tilde{u}(n+1) &= a_1\tilde{u}(n) + a_2\tilde{v}(n) + a_{11}\tilde{u}^2(n) + a_{12}\tilde{u}(n)\tilde{v}(n) + a_{22}\tilde{v}^2(n) + O((|\tilde{u}(n)| + |\tilde{v}(n)|)^3), \\ \tilde{v}(n+1) &= b_1\tilde{u}(n) + b_2\tilde{v}(n) + b_{11}\tilde{u}^2(n) + b_{12}\tilde{u}(n)\tilde{v}(n) + b_{22}\tilde{v}^2(n) + O((|\tilde{u}(n)| + |\tilde{v}(n)|)^3). \end{aligned} \tag{2.11}$$

We specifically reference the crucial parameters a_1, a_2, b_1, and b_2 defined i Appendix. Furthermore, the essential values $a_{11}, a_{12}, a_{22}, b_{11}$, and b_{12} are clearly defined in Appendix.
The Jacobian matrix of model (2.10) at the equilibrium point E_2 is defined as follows:

$$J_1(\tilde{r}, \tilde{\eta}) = \begin{pmatrix} 1 + x^*\Big[\frac{\tilde{r}(Ak - x^{*2} - 2Ax^*)}{k(x^*+A)^2} + \frac{y^*(a-a\beta+\alpha\omega)(1-\beta+qm))}{(1+x^*(1-\beta+qm))^2}\Big] & \frac{-x^*(a-a\beta+\alpha\omega)}{1+x^*(1-\beta+qm)} \\ \frac{\tilde{\eta}y^*(a-a\beta+\alpha\omega)}{(1+x^*(1-\beta+qm))^2}, & 1 \end{pmatrix}.$$

Additionally, we calculate a pair of adjoint eigenvectors, $q(\tilde{r}, \tilde{\eta})$ and $q(\tilde{r}, \tilde{\eta}) \in \mathbb{C}$, ensuring they satisfy the following relationships:
$J_1(\tilde{r}, \tilde{\eta})q(\tilde{r}, \tilde{\eta}) = \frac{-1+\sqrt{3}i}{2}q(\tilde{r}, \tilde{\eta})$, $J_1^T(\tilde{r}, \tilde{\eta})p(\tilde{r}, \tilde{\eta}) = -\frac{1+\sqrt{3}i}{2}p(\tilde{r}, \tilde{\eta})$,
$\langle p(\tilde{r}, \tilde{\eta}), q(\tilde{r}, \tilde{\eta})\rangle = 1$, where $\langle ., .\rangle$ is the standard scalar product in $\mathbb{C}$: $\langle p, q\rangle = \bar{p_1}q_1 + \bar{p_2}q_2$. Once we've done some math, we can make an assessment:

$$q(\tilde{r}, \tilde{\eta}) = \begin{pmatrix} \frac{x^*(a-a\beta+\alpha\omega)}{1+x^*(1-\beta+qm)} \\ \frac{3-\sqrt{3}i}{2} + \frac{rx^*(Ak-x^{*2}-2Ax^*)(1+x^*(1-\beta+qm))^2 + kx^*y^*(A+x^*)^2(a-a\beta+\alpha\omega)(1-\beta+qm)}{k(A+x^*)^2(1+x^*(1-\beta+qm))^2} \end{pmatrix},$$

$$p(\tilde{r}, \tilde{\eta}) = \begin{pmatrix} \frac{(\sqrt{3}i-1)(1+x^*(1-\beta+qm))}{2x^*(a-a\beta+\alpha\omega)} \\ \frac{\sqrt{3}i}{3} \end{pmatrix}.$$

For any vector $x \in \mathbb{R}^2$, the expression can be determined as follows

$$x_n = zq(\tilde{r}, \tilde{\eta}) + \bar{z}\overline{q(\tilde{r}, \tilde{\eta})}, z \in \mathbb{C}.$$

Map (2.11) can be converted into its complex form.

$$z \to \frac{\sqrt{3}i - 1}{2}z + \sum_{2\le l+k\le 3} \frac{1}{k!l!}g_{kl}z^k\bar{z}^l, \tag{2.12}$$

where

$$
\begin{cases}
g_{20}(r,\eta) = \frac{1}{k(A+x^*)^2(1+x^*-x^*\beta+qmx^*)^2}\Big[2ix^*\eta(a(-1+\beta)-\alpha\omega(x^*y^*(-1+\beta-qm) \\
\quad -(a(-1+\beta)-\alpha\omega)^2(-2+2x^*(-1+\beta-qm)+a\eta(-1+\beta)-\alpha\eta\omega)-(1+x^*-x^*\beta \\
\quad +qmx^*)^3(a-a\beta+\alpha\omega) \\
\quad \Big(\frac{3}{2}-\frac{\sqrt{3}i}{2}+rx^*(A(k-2x^*)-x^{*2})(1+x^*-x^*\beta+qmx^*)^2+kx^*y^*((A+x^*)^2(1-\beta \\
\quad +qm)(a-a\beta+\alpha\omega))))\Big)\Big] \\
\quad +\frac{1}{k(A+x^*)^2(1+x^*-x^*\beta+qmx^*)^2}\Big((-1+\sqrt{3}i)y^*(1+x^*-x^*\beta+qmx^*)((a-a\beta+\alpha\omega)^2)(\frac{3}{2}-\frac{\sqrt{3}i}{2} \\
\quad +rx^*(A(k-2x^*)-x^{*2})(1+x^*-x^*\beta+qmx^*)^2+kx^*y^*((A+x^*)^2(1-\beta+qm)(a-a\beta \\
\quad +\alpha\omega)))\Big)^2 \\
\quad +\frac{1}{k(A+x^*)^2(1+x^*-x^*\beta+qmx^*)^2}\Big((\frac{3}{2}-\frac{\sqrt{3}i}{2}+rx^*(A(k-2x^*)-x^{*2})(1+x^*-x^*\beta+qmx^*)^2 \\
\quad +kx^*y^*((A+x^*)^2(1-\beta+qm)(a-a\beta+\alpha\omega)))\Big), \\
\\
g_{11}(r,\eta) = \frac{1}{\sqrt{3}(1+x^*-x^*\beta+qmx^*)^3}\Big(2ix^*\eta(a(-1+\beta)-\alpha\omega(x^*y^*(-1+\beta-qm) \\
\quad -(a(-1+\beta)-\alpha\omega)^2(-2+2x^*(-1+\beta-qm)+a\eta(-1+\beta)-\alpha\eta\omega) \\
\quad -(1+x^*-x^*\beta+qmx^*)^3(a-a\beta \\
\quad +\alpha\omega)\Big(\frac{rx^*(A(k-2x^*)-x^{*2})(1+x^*-x^*\beta+qmx^*)^2+kx^*y^*((A+x^*)^2(1-\beta+qm)(a-a\beta+\alpha\omega))}{k(A+x^*)^2(1+x^*-x^*\beta+qmx^*)^2} \\
\quad -\frac{3}{2}-\frac{\sqrt{3}i}{2}\Big)+x^{*2}(1+x^*-x^*\beta+qmx^*)(a(-1+\beta) \\
\quad +\alpha\omega)^2\Big(\frac{y^*(1-\beta+qm)(1+x^*(-1+\beta-qm))(a-a\beta+\alpha\omega)}{(1+x^*-x^*\beta+qmx^*)^3} \\
\quad +\frac{r(A^2(k-4x^*)-Akx^*-x^{*3})}{k(A+x^*)^3}\Big), \\
\\
g_{02}(r,\eta) = \frac{1}{2\sqrt{3}(1+x^*-x^*\beta+qmx^*)^3}\Big(2ix^*\eta(a(-1+\beta)-\alpha\omega(x^*y^*(-1+\beta-qm) \\
\quad -(a(-1+\beta)-\alpha\omega)^2(-2+2x^*(-1+\beta-qm)+a\eta(-1+\beta)-\alpha\eta\omega) \\
\quad -(1+x^*-x^*\beta+qmx^*)^3(a-a\beta \\
\quad +\alpha\omega)\Big(\frac{rx^*(A(k-2x^*)-x^{*2})(1+x^*-x^*\beta+qmx^*)^2+kx^*y^*((A+x^*)^2(1-\beta+qm)(a-a\beta+\alpha\omega))}{k(A+x^*)^2(1+x^*-x^*\beta+qmx^*)^2} \\
\quad -\frac{3}{2}-\frac{\sqrt{3}i}{2}\Big)+\Big(x^*(-1+\beta-qm)+(1+x^*-x^*\beta+qmx^*)\Big)\Big(1+x^*(\frac{r(A(k-2x^*)x^{*2})}{k(A+x^*)^2})\Big) \\
\quad +\frac{y^*((1-\beta+qm)(a-a\beta+\alpha\omega))}{(1+x^*-x^*\beta+qmx^*)^2}\Big) \\
\quad +x^{*2}(1+x^*-x^*\beta+qmx^*)(a(-1+\beta)+\alpha\omega)^2\Big(\frac{y^*(1-\beta+qm)(1+x^*(-1+\beta-qm))(a-a\beta+\alpha\omega)}{(1+x^*-x^*\beta+qmx^*)^3} \\
\quad +\frac{r(A^2(k-4x^*)-Akx^*-x^{*3})}{k(A+x^*)^3}\Big), \\
\\
g_{30}(r,\eta) = g_{12}(r,\eta) = g_{21}(r,\eta) = g_{03}(r,\eta) = 0.
\end{cases}
$$

To remove all quadratic terms, implement the subsequent transformation:

$$z = \phi + \frac{1}{2}h_{20}\phi^2 + h_{11}\phi\overline{\phi} + \frac{1}{2}h_{02}\overline{\phi}^2, \tag{2.13}$$

Transformation (2.13) and its inverse transformation are used to change Map (2.12) into

$$\phi \to \frac{\sqrt{3}i-1}{2}\phi + \sum_{2\leq l+k\leq 3}\frac{1}{k!l!}\varrho_{kl}\phi^k\overline{\phi}^l + O(|\phi|^4), \tag{2.14}$$

where

$$\varrho_{20} = g_{20} + \sqrt{3}ih_{20},\ \varrho_{11} = 2g_{11} + (\sqrt{3}i-3)h_{11} \text{ and } \varrho_{02} = g_{02}.$$

By setting

$$h_{20} = \frac{\sqrt{3}i}{3}g_{20},\ h_{11} = \frac{3+\sqrt{3}i}{6}g_{11} \text{ and } h_{02} = 0.$$

Based on the earlier values of ϱ and h, we determine that $\varrho_{20} = \varrho_{11} = 0$, while ϱ_{02} equals g_{02}. Additionally, the expressions for $\varrho_{30}, \varrho_{21}, \varrho_{12}$, and ϱ_{03} can be simplified as follows:

$$\begin{cases} \varrho_{30} = \frac{3-\sqrt{3}i}{2}g_{11}\overline{g}_{02} + \sqrt{3}ig_{20}^2 + g_{30}, \\ \varrho_{21} = \frac{3+2\sqrt{3}i}{2}g_{11}g_{20} + \frac{3-\sqrt{3}i}{3}|g_{11}|^2 + g_{21}, \\ \varrho_{12} = \frac{3+\sqrt{3}i}{6}g_{20}g_{02} + \frac{3-\sqrt{3}i}{3}\overline{g}_{11}g_{02} + \frac{3+\sqrt{3}i}{3}g_{11}^2 - \frac{\sqrt{3}i}{3}\overline{g}_{20}g_{11}, \\ \varrho_{03} = \sqrt{3}ig_{11}g_{02} - \sqrt{3}ig_{02}\overline{g}_{20} + g_{03}. \end{cases}$$

To simplify Equation (2.14), we proceed by applying the following transformation:

$$\phi = \epsilon + \frac{1}{6}h_{30}\epsilon^3 + \frac{1}{2}h_{21}\epsilon^2\overline{\epsilon} + \frac{1}{2}h_{12}\epsilon\overline{\epsilon}^2 + \frac{1}{6}h_{03}\overline{\epsilon}^3. \tag{2.15}$$

By applying Equation (2.15) along with its inverse, Map (2.14) is derived as follows.

$$\epsilon = \frac{\sqrt{3}i-1}{2}\epsilon + \frac{1}{2}g_{02}\overline{\epsilon}^2 + \sum_{l+k=3}\frac{1}{k!l!}\tilde{\varrho}_{kl}\epsilon^k\overline{\epsilon}^l + O(|\epsilon|^4), \tag{2.16}$$

where

$$\tilde{\varrho}_{30} = \varrho_{30} + \frac{\sqrt{3}i-3}{2}h_{30},\ \tilde{\varrho}_{21} = \varrho_{21},$$

$$\tilde{\varrho}_{12} = \varrho_{12} + \sqrt{3}ih_{12} \text{ and } \tilde{\varrho}_{03} = \varrho_{03} + \frac{\sqrt{3}i-3}{2}h_{03}.$$

By putting

$$h_{30} = \frac{3+\sqrt{3}i}{6}\varrho_{30},\ h_{12} = \frac{\sqrt{3}i}{3}\varrho_{12}, h_{03} = \frac{3+\sqrt{3}i}{6}\varrho_{03} \text{ and } h_{21} = 0.$$

Next, we have $\tilde{\varrho}_{30} = \tilde{\varrho}_{21} = \tilde{\varrho}_{03} = 0$.

Finally, the typical form of the bifurcation that exhibits a 1:3 resonance is presented in the following way:

$$\epsilon \to \frac{\sqrt{3}i-1}{2}\epsilon + B(\tilde{r},\tilde{\eta})\bar{\epsilon} + C(\tilde{r},\tilde{\eta})\epsilon|\epsilon|^2 + O(|\epsilon|^4), \tag{2.17}$$

where

$$B(\tilde{r},\tilde{\eta}) = \frac{1}{2}g_{02}(r,\eta),\ C(\tilde{r},\tilde{\eta}) = \frac{(3+\sqrt{3}i)g_{20}g_{11}}{6} + \frac{(3-\sqrt{3}i)|g_{11}|^2}{6} + \frac{1}{2}g_{21}.$$

If

$$B_1(\tilde{r},\tilde{\eta}) = \frac{-3}{2}(\sqrt{3}i+1)B(\tilde{r},\tilde{\eta}),$$
$$C_1(\tilde{r},\tilde{\eta}) = -3|B(\tilde{r},\tilde{\eta})|^2 - \frac{3}{2}(\sqrt{3}i+1)C(\tilde{r},\tilde{\eta}).$$

The following theorem can be demonstrated by making use of Lemma (9.11) and Lemma (9.13) as they are presented in [23]:

Theorem 2.2. *If $B_1(\tilde{r},\tilde{\eta}) \neq 0$ and $Re(C_1(\tilde{r},\tilde{\eta})) \neq 0$, then Map (1.1) shows a number of interesting and complex dynamical actions at the fixed point E^*.*

- *In map (2.17), a Neimark-Sacker bifurcation occurs at the trivial fixed point E_1.*
- *A three-period saddle cycle is connected with the fixed point $E_k(k=1,2,3)$ in map (2.17).*
- *The period-3 cycle's stable and unstable invariant manifolds come together to make a homoclinic structure. The points where their transversal axes meet are limited in a way that gets smaller and smaller.*

Remark 2.2. *In a 1:3 resonance, stable and unstable manifolds interact, producing an infinite series of period-three orbits and leading to a homoclinic tangency. This tangency is not just an unusual mathematical problem, but it also signifies chaotic dynamics. Complex dynamics, characterized by a deterministic disorder, employs saddle orbit period-three cycles. Non-degenerate Neimark–Sacker bifurcations serve as thresholds for quasi-periodic and chaotic oscillations, illustrating this occurrence in biological systems, particularly those with interacting populations and constrained resources. Period-three oscillations indicate chaotic sets—strange attractors that dictate irregular yet structured long-term behavior, rather than the system itself. In a nonlinear environment, the homoclinic structure responsible for these phenomena induces population surges, declines, and disorder.*

2.3. **The 1:4 strong resonance of model (1.1) at the Positive Fixed Point $E_2(x^*,y^*)$.** This work elucidates the 1:4 resonance of model (1.1) at the positive fixed point $E_2(x^*,y^*)$ when parameters r and η vary within a narrow range of F_{14}. Furthermore, the parameters $(\check{r},A,k,a,\beta,\alpha,\omega,m,q,\check{\eta},\mu)$ are chosen arbitrarily from F_{14}, with $\check{r}$ and $\check{\eta}$ regarded as bifurcation parameters. Model (1.1) with parameters $(\check{r},A,k,a,\beta,\alpha,\omega,m,q,\check{\eta},\mu)$ is articulated as follows:

$$\begin{aligned} x(n+1) &= x(n)exp\Big[\check{r}(1-\frac{x(n)}{k})(\frac{x(n)}{x(n)+A}) - \frac{y(n)(a(1-\beta)+\alpha\omega)}{1+x(n)(1-\beta+qm)}\Big], \\ y(n+1) &= y(n)exp\Big[\frac{\check{\eta}x(n)(a(1-\beta)+\alpha\omega)}{1+x(n)(1-\beta+qm)} - \mu\Big], \end{aligned} \tag{2.18}$$

where $|r-\check{r}|, |\eta-\check{\eta}| \ll 1$, and the eigenvalues of model (2.18) at the positive equilibrium point are $\lambda_{1,2} = \pm i$.

Let $\check{u} = x - x^*$ and $\check{v} = y - y^*$. By shifting the reference frame to place the point $E_2(x^*, y^*)$ at the origin, the transformation maps (x^*, y^*) into $(\check{u}, \check{v})$. Consequently, the updated form of map (2.18) is redefined within this new coordinate system as

$$\begin{aligned} \check{u}(n+1) &= a_1\check{u}(n) + a_2\check{v}(n) + a_{11}\check{u}^2(n) + a_{12}\tilde{u}(n)\check{v}(n) + a_{22}\tilde{v}^2(n) + O((|\tilde{u}(n)| + |\check{v}(n)|)^3), \\ \check{v}(n+1) &= b_1\check{u}(n) + b_2\check{v}(n) + b_{11}\check{u}^2(n) + b_{12}\check{u}(n)\check{v}(n) + b_{22}\check{v}^2(n) + O((|\check{u}(n)| + |\check{v}(n)|)^3), \end{aligned} \tag{2.19}$$

the parameters a_1, a_2, b_1, and b_2 are specified in Appendix. Similarly, $a_{11}, a_{12}, a_{22}, b_{11}$, and b_{12} are explicitly defined in Appendix.

At the point $E_2(\check{r}, \check{\eta})$, the Jacobian matrix for model (2.18) is defined as follows:

$$J_2(\check{r}, \check{\eta}) = \begin{pmatrix} 1 + x^*\Big[\frac{\check{r}(Ak - x^{*2} - 2Ax^*)}{k(x^*+A)^2} + \frac{y^*(a-a\beta+\alpha\omega)(1-\beta+qm)}{(1+x^*(1-\beta+qm))^2}\Big] & \frac{-x^*(a-a\beta+\alpha\omega)}{1+x^*(1-\beta+qm)} \\ \frac{\check{\eta}y^*(a-a\beta+\alpha\omega)}{(1+x^*(1-\beta+qm))^2}, & 1 \end{pmatrix}.$$

Moreover, we can obtain a pair of adjoint eigenvectors, $q(\check{r}, \check{\eta}) and p(\check{r}, \check{\eta}) \in \mathbb{C}$, such that

$J_2(\check{r}, \check{\eta})q(\check{r}, \check{\eta}) = iq(\check{r}, \check{\eta}),\ J_2^T(\check{r}, \check{\eta})p(\check{r}, \check{\eta}) = -ip(\check{r}, \check{\eta}),\ \langle p(\check{r}, \check{\eta}), q(\check{r}, \check{\eta})\rangle = 1.$

According to our prior exchanges, we possess the following information:

$$q(\check{r}, \check{\eta}) = \begin{pmatrix} \frac{x^*(a-a\beta+\alpha\omega)}{1+x^*(1-\beta+qm)} \\ 1 - i + \frac{rx^*(Ak-x^{*2}-2Ax^*)(1+x^*(1-\beta+qm))^2 + kx^*y^*(A+x^*)^2(a-a\beta+\alpha\omega)(1-\beta+qm)}{k(A+x^*)^2(1+x^*(1-\beta+qm))^2} \end{pmatrix},$$

$$p(\check{r}, \check{\eta}) = \begin{pmatrix} \frac{(i-1)(1+x^*(1-\beta+qm))}{2x^*(a-a\beta+\alpha\omega)} \\ \frac{i}{2} \end{pmatrix}.$$

For any vector $Y_n = (\check{u}, \check{v})^T \in \mathbb{R}^2$, it can be expressed as

$$Y_n = zq(\check{r}, \check{\eta}) + \bar{z}\bar{q}(\check{r}, \check{\eta}), z \in \mathbb{C}.$$

Then, model (2.19) evolves into the following intricate relationship:

$$z \longmapsto iz + \sum_{2 \le k+l \le 3} \frac{1}{k!l!} g_{kl} z^k \bar{z}^l, \tag{2.20}$$

where

$$
\begin{cases}
g_{20} = i\Big[\frac{1}{k(A+x^*)^2(1+x^*-x^*\beta+qmx^*)^2}\Big(2x^{*2}y^*\eta(-1+\beta-qm)(a(-1+\beta)-\alpha\omega)^3 \\
(-2+2x^*(-1+\beta-qm)+a\eta(-1+\beta)-\alpha\eta\omega)-2x^*\eta(-1+x^*-x^*\beta+qm)^3 \\
(a(-1+\beta)-\alpha\omega)(a-a\beta+\alpha\omega)\Big((1-i)+(rx^*(A(k-2x^*)-x^{*2})(1+x^*-x^*\beta+qmx^*)^2 \\
+kx^*y^*(A+x^*)^2(1-\beta-qm)(a-a\beta+\alpha\omega))\Big)\Big)+2(1+x^*-x^*\beta+qmx^*)^3((1+i) \\
+\frac{(1+x^*-x^*\beta+qmx^*)}{x^*(a-a\beta+\alpha\omega)}) \\
(y^*(1+x^*-x^*\beta+qmx^*)(a-a\beta+\alpha\omega)^2)\Big((1-i)+(rx^*(A(k-2x^*)-x^{*2}) \\
(1+x^*-x^*\beta+qmx^*)^2+kx^*y^*(A+x^*)^2(1-\beta-qm)(a-a\beta+\alpha\omega))\Big)^2\Big], \\
\\
g_{11} = i\Big[\frac{1}{k(A+x^*)^2(1+x^*-x^*\beta+qmx^*)^2}\Big(2x^{*2}y^*\eta(-1+\beta-qm)(a(-1+\beta)-\alpha\omega)^3 \\
(-2+2x^*(-1+\beta-qm)+a\eta(-1+\beta)-\alpha\eta\omega)-2x^*\eta(-1+x^*-x^*\beta+qm)^3 \\
(a(-1+\beta)-\alpha\omega)(a-a\beta+\alpha\omega)\Big((1-i)+(rx^*(A(k-2x^*)-x^{*2})(1+x^*-x^*\beta+qmx^*)^2 \\
+kx^*y^*(A+x^*)^2(1-\beta-qm)(a-a\beta+\alpha\omega))\Big)\Big)+2(1+x^*-x^*\beta+qmx^*)^3((1+i) \\
+\frac{(1+x^*-x^*\beta+qmx^*)}{x^*(a-a\beta+\alpha\omega)}) \\
(y^*(1+x^*-x^*\beta+qmx^*)(a-a\beta+\alpha\omega)^2)\Big((1-i)+(rx^*(A(k-2x^*)-x^{*2}) \\
(1+x^*-x^*\beta+qmx^*)^2+kx^*y^*(A+x^*)^2(1-\beta-qm)(a-a\beta+\alpha\omega))\Big)^2 \\
+\frac{1}{2(1+x^*-x^*\beta+qmx^*)^6}\Big(1+x^*(\frac{r(A(k-2x^*)-x^{*2})}{k(A+x^*)^2}+\frac{y^*(-1+\beta-qm)(a-a\beta+\alpha\omega)}{(1+x^*-x^*\beta+qmx^*)^2})\Big)\Big], \\
\\
g_{02} = i\Big[\frac{1}{k(A+x^*)^2(1+x^*-x^*\beta+qmx^*)^2}\Big(2x^{*2}y^*\eta(-1+\beta-qm)(a(-1+\beta)-\alpha\omega)^3 \\
(-2+2x^*(-1+\beta-qm)+a\eta(-1+\beta)-\alpha\eta\omega)-2x^*\eta(-1+x^*-x^*\beta+qm)^3 \\
(a(-1+\beta)-\alpha\omega)(a-a\beta+\alpha\omega)\Big((1-i)+(rx^*(A(k-2x^*)-x^{*2})(1+x^*-x^*\beta+qmx^*)^2 \\
+kx^*y^*(A+x^*)^2(1-\beta-qm)(a-a\beta+\alpha\omega))\Big)\Big)+2(1+x^*-x^*\beta+qmx^*)^3((1+i) \\
+\frac{(1+x^*-x^*\beta+qmx^*)}{x^*(a-a\beta+\alpha\omega)}) \\
(y^*(1+x^*-x^*\beta+qmx^*)(a-a\beta+\alpha\omega)^2)\Big((1-i)+(rx^*(A(k-2x^*)-x^{*2}) \\
(1+x^*-x^*\beta+qmx^*)^2+kx^*y^*(A+x^*)^2(1-\beta-qm)(a-a\beta+\alpha\omega))\Big)^2 \\
\Big(x^*(-1+\beta-qm)+(1+x^*-x^*\beta+qmx^*)\Big(1+x^*(\frac{r(A(k-2x^*)-x^{*2})}{k(A+x^*)^2} \\
+\frac{y^*(-1+\beta-qm)(a-a\beta+\alpha\omega)}{(1+x^*-x^*\beta+qmx^*)^2})\Big) \\
+x^{*2}(1+x^*-x^*\beta+qmx^*)((a(-1+\beta)-\alpha\omega)^2)\Big], \\
\\
g_{30} = g_{12} = g_{21} = g_{03} = 0.
\end{cases}
$$

To efficiently eradicate the quadratic terms, we offer the subsequent equation:

$$z = \gamma + \frac{1}{2}h_{20}\gamma^2 + h_{11}\gamma\bar{\gamma} + \frac{1}{2}h_{02}\bar{\gamma}^2, \tag{2.21}$$

The coefficients h_{kl}, relevant when $k+l=2$, are specified in the subsequent relation. By employing Transformation (2.21) and its inverse, Map (2.20) can be restructured as follows.

$$\gamma \longmapsto i\gamma + \sum_{2\leq k+l\leq 3} \frac{1}{k!l!}\varrho_{kl}\gamma^k\bar{\gamma}^l + O((|\gamma|+|\bar{\gamma}|)^4), \tag{2.22}$$

where

$$\begin{cases} \varrho_{20} = \frac{1}{2}(g_{20} + (\lambda - \lambda^2)h_{20}),\ \varrho_{11} = g_{11} + (\lambda - |\lambda|^2)h_{11}, \\ \varrho_{20} = \frac{1}{2}(g_{02} + (\lambda - \bar{\lambda}^2)h_{02}),\ \varrho_{30} = \frac{1}{6}(g_{30} + (\lambda - \lambda^3)h_{30}), \\ \varrho_{21} = \frac{1}{2}(g_{21} + (\lambda - \lambda|\lambda|^2)h_{21}),\ \varrho_{12} = \frac{1}{2}(g_{12} + (\lambda - \bar{\lambda}|\lambda|^2)h_{12}), \\ \varrho_{03} = \frac{1}{6}(g_{03} + (\lambda - \bar{\lambda}^3)h_{03}). \end{cases}$$

By setting

$h_{20} = \frac{1}{2}(i-1)g_{20},\ h_{11} = \frac{1}{2}(i+1)g_{11},\ h_{02} = \frac{1}{2}(i+1)g_{02}$,

then, we get $\varrho_{20} = \varrho_{11} = \varrho_{02} = 0$.

To diminish certain cubic terms, we recommend executing the subsequent transformation:

$$\gamma = \zeta + \frac{1}{6}h_{30}\zeta^3 + \frac{1}{2}h_{21}\zeta^2\bar{\zeta} + \frac{1}{2}h_{12}\zeta\bar{\zeta}^2 + \frac{1}{3}h_{03}\bar{\zeta}^3. \tag{2.23}$$

Utilizing Equation (2.23) and its inverse transformation, we obtain the subsequent results:

$$\gamma \mapsto i\zeta + \sum_{k+l=3} \frac{1}{k!l!}\bar{\varrho}_{kl}\zeta^k\bar{\zeta}^l + O(|\bar{\zeta}|)^4, \tag{2.24}$$

where

$$\bar{\varrho}_{30} = \varrho_{30} + 2i\bar{h}_{30},\ \bar{\varrho}_{21} = \varrho_{21},$$
$$\bar{\varrho}_{12} = \varrho_{12} + 2i\bar{h}_{12},\ \bar{\varrho}_{03} = \varrho_{03}.$$

Let

$$h_{30} = \frac{i}{2}\varrho_{30},\ h_{12} = \frac{i}{2}\varrho_{12},\ h_{03} = h_{21} = 0,$$

From the above relationship, we conclude that $\bar{\varrho}_{30} = \bar{\varrho}_{12} = 0$. Ultimately, at the 1:4 resonance point, model (2.24) can be reformulated as:

$$\zeta \to i\zeta + C(\check{r},\check{\eta})\zeta|\zeta|^2 + D(\check{r},\check{\eta})|\bar{\zeta}|^3 + O(|\zeta|)^4, \tag{2.25}$$

where

$$C(\check{r},\check{\eta}) = ig_{11}^2 - \frac{1}{2}g_{11}\bar{g}_{20}(1+i) + \bar{g}_{11}g_{02} + g_{02}g_{11}(i-1) - \frac{1}{2}g_{11}g_{20}(1-2i),$$
$$D(\check{r},\check{\eta}) = \frac{i-1}{4}g_{02}g_{11} - \frac{i+1}{4}g_{20}g_{11} + \frac{1}{6}g_{03}.$$

Let $C_1(\check{r},\check{\eta}) = -4iC(\check{r},\check{\eta})$, $D_1(\check{r},\check{\eta}) = -4iD(\check{r},\check{\eta})$. When $D_1 \neq 0$, we coclude that

$A(\check{r},\check{\eta}) = \frac{C_1(\check{r},\check{\eta})}{|D_1(\check{r},\check{\eta})|}$.

Theorem 2.3. *Consider the case where* $(\check{r}, \check{\eta}) \in F_{14}$. *If* $ReA(\check{r}, \check{\eta}) \neq 0$ *and* $ImA(\check{r}, \check{\eta}) \neq 0$, *model (1.1) demonstrates a rich variety of dynamical behaviors (refer to [23]):*

(1) *Notably, a Neimark–Sacker bifurcation curve emerges at the trivial fixed point* E_1 *as shown in equation (2.25). Furthermore, for* $\lambda = -i$, *an invariant circle is present; however, this circle vanishes when* $\lambda = i$.
(2) *When* $|A| > 1$, *System (2.25) features eight non-trivial equilibrium points, labeled* S_k*and*E_k *where* $k = 1, 2, 3, 4$. *These eight non-trivial fixed points can either appear or disappear at specific parameter values during a fold bifurcation.*
(3) *Additionally, Neimark–Sacker bifurcations occur at each fixed point* E_k *for* $k = 1, 2, 3, 4$, *highlighting the intricate behavior of the system under varying conditions.*

Remark 2.3. *In nonlinear dynamics, a nondegenerate Neimark–Sacker bifurcation starts at a 1:4 resonance. A closed invariant curve from stable equilibrium creates four-period waves. Transition from static to ordered periodicity in biological systems, especially those with limited resources and populations. Resource and population changes cycle four times. Built-in delays and feedback loops oscillate. They have complex ecological interactions like overshoot, collapse, and rebound. The system is limited and sensible independent of cycle period. Natural stability often resembles dynamic balance.*

3. Numerical Continuation

In this section we do a numerical bifurcation analysis using the MATLAB software MATCONTM [33]. The study uses continuation methods to track the solution manifolds of fixed points under variations of the map's parameters. In a two-parameter setting, the domains of cycle-stability are commonly described in terms of bifurcation curves obtained via MATCONTM. The bifurcation curves cannot be obtained analytically and have to be estimated using numerical continuation methods.

Example 3.1. *In this example, we run the numerical continuation of the positive fixed point* $E_2(x^*, y^*) = (4.29997, 14.054)$. *The parameters are set to* $k = 10, A = 2, a = 0.2, \beta = 0.4, \alpha = 0.2, \omega = 0.4, q = 0.2, m = 0.02, r = 3, \mu = 0.1$, *and* η *is a bifurcation parameter. Figure 1 clearly indicates that the positive fixed point E2 becomes unstable when a subcritical Neimark-Sacker bifurcation (NS) happens at* $\eta = 0.399135$. *Also, at* $\eta = 0.357048$, *a subcritical period-doubling bifurcation happens at* E_2, *which is designated as PD. There is also a branch point at* $\eta = 0.352000$, *which is called BP.*

Example 3.2. *We look at the dynamics with* η *going from 0.357 to 0.372, using the same parametric settings as in example (3.1). Two-cycle dynamics emerge at the PD point of model (1.1). Using the continuation method, we can easily move to this 2-cycle, which eventually becomes unstable because of a supercritical PD bifurcation. For a more in-depth look, see the associated MATCONT report in [33]. When* η *is greater than* 0.369362, *a stable 4-cycle can form. Also, when* η *is greater than* 0.371791, *a stable 8-cycle appears, which is defined as* $(C_8 = X_1, \ldots, X_8)$, *where* $(X_1 = (4.29997, 14.054))$, *and* $\eta = 0.357048$. *Two species live*

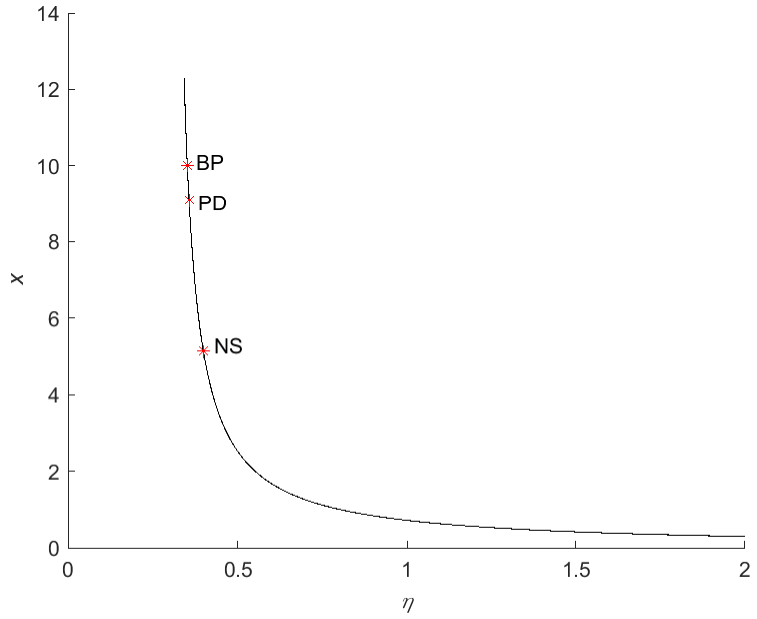


FIGURE 1. Continuation curve of E^* in (η, x)-plane. The Neimark-Sacker point (NS), period doubling point (PD) and branch point (BP).

together here and go through their cycles every eight time intervals. Figure 2 clearly shows the PD points for the second and fourth iterations, and Figure 3 clearly shows the 4-cycle and 8-cycle points.

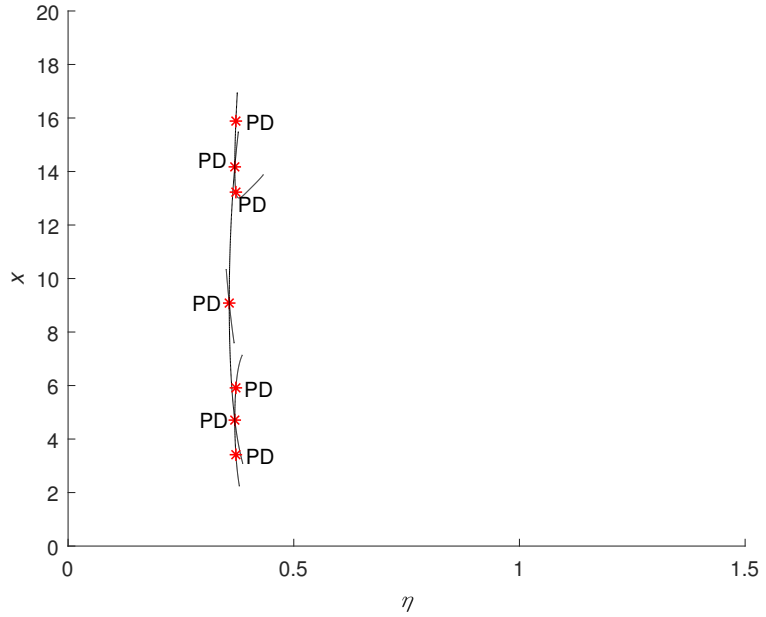
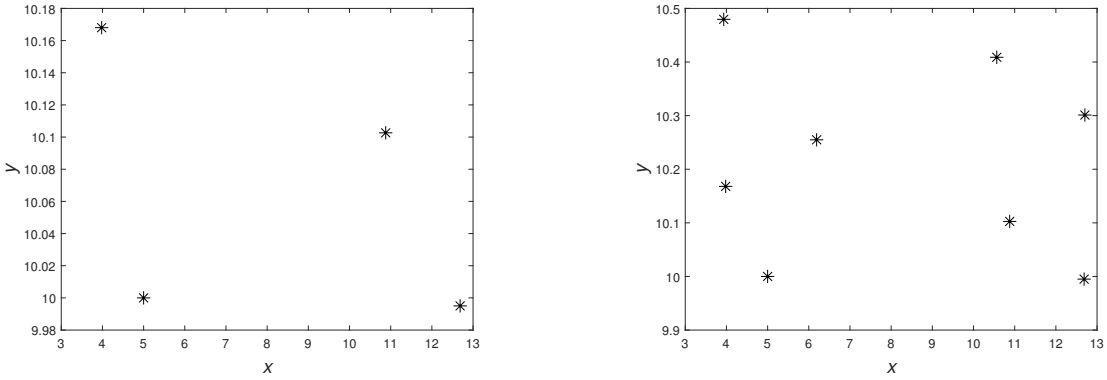


FIGURE 2. First, second and fourth iterates for fixed point curves in the plane (η, x).



(A) (B)

FIGURE 3. (a) A stable 4-cycle of model (1.1) for $\eta = 0.394$. (b) A stable 8-cycle for $\eta = 0.4$.

Example 3.3. *In this instance, we examine the essential evaluation of codimension-2 bifurcations. We commence our investigation by determining the period-doubling curve (PD), beginning at the specified period-doubling (PD) point. We set the values of the parameters to* $k = 10, A = 2, a = 0.2, \beta = 0.4, \alpha = 0.2, \omega = 0.4, q = 0.2, m = 0.1,$ *and* $\mu = 0.1$. *This lets us change r and* η *to look at different situations. The MATCONT report that goes with this is easy to find in [33]. It is important to know that the codimension-2 bifurcations along this period-doubling curve include important events like the fold-flip (LPPD) and generalized period doubling (GPD). Figure 4 shows the calculated period-doubling curve in a very clear way.*

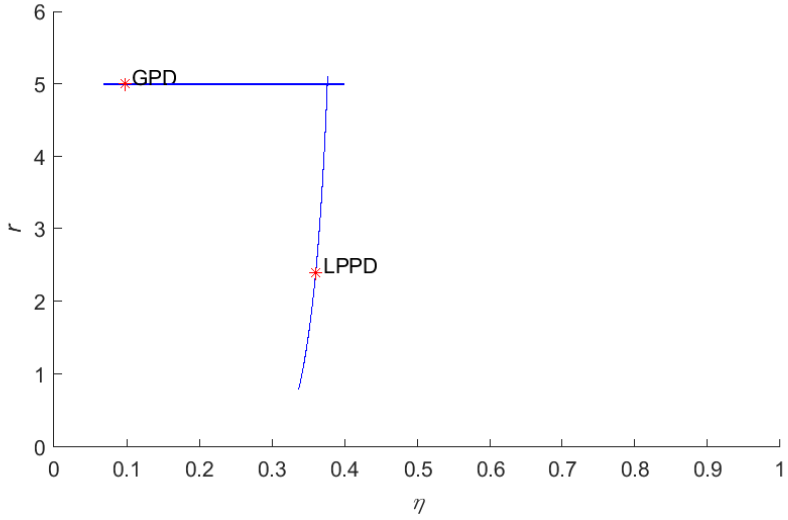


FIGURE 4. Period-doubling curve, including GPD point, and LPPD point rooted at the PD point.

4. Conclusion

In this paper, we thoroughly investigated codimension-two bifurcations, with a focus on the 1:2, 1:3 and 1:4 resonances. We derived explicit criteria to distinguish subcritical bifurcations (associated with unstable limit cycles) from supercritical ones using a rigorous analytical framework based on normal-form theory and center-manifold reduction. Extensive numerical simulations, including continuation and stability assessments, supported the theoretical predictions with good quantitative accuracy in all resonance scenarios . This close match supports the suggested reduction approach and illustrates the predictive reliability of the approach for anticipating bifurcation-induced instabilities in practical applications. These results provide a solid basis for expanding this paradigm to higher-order resonances, stochastic systems, or time-delayed dynamical regimes in future study.

Appendix

The expressions of $a_{11}, a_{12}, a_{22}, a_{111}, a_{112}, a_{112}, a_{221}, a_{222}, b_{12}$, and b_{112} are defined as follows:

$$\begin{cases} a_{11} = \frac{1}{2}\Bigg[\Big(\frac{r(Ak-2Ax^*-x^{*2})}{k(x^*+A)^2} + \frac{y^*(a-a\beta+\alpha\omega)(1-\beta+qm)}{(1+x^*(1-\beta+qm))^2}\Big)\Big(1 + \frac{rx^*(Ak-2Ax-x^{*2})}{k(x^*+A)^2} + \frac{x^*y^*(a-a\beta+\alpha\omega)(1-\beta+qm)}{(1+x^*(1-\beta+qm))^2}\Big) \\ \qquad + \frac{A^2rk-rx^{*3}-4A^2rx^*-Arkx^*}{k(x^*+A)^3} + \frac{y^*(a-a\beta+\alpha\omega)(1-\beta+qm)(1-x^*(1-\beta+qm))}{(1+x^*(1-\beta+qm))^3}\Bigg], \\ a_{12} = \frac{x^*(a-a\beta+\alpha\omega)(1-\beta+qm)}{(1+x^*(1-\beta+qm))^2} - \Big(\frac{a-a\beta+\alpha\omega}{1+x^*(1-\beta+qm)}\Big)\Big(1 + \frac{rx^*(Ak-2Ax-x^{*2})}{k(x^*+A)^2} + \frac{x^*y^*(a-a\beta+\alpha\omega)(1-\beta+qm)}{(1+x^*(1-\beta+qm))^2}\Big), \\ a_{22} = \frac{x^*(a-a\beta+\alpha\omega)^2}{2(1+x^*(1-\beta+qm))^2}, \end{cases}$$

$$\begin{cases} a_{111} = \frac{1}{6}\Bigg[\Big(1 + \frac{rx^*(Ak-2Ax-x^{*2})}{k(x^*+A)^2} + \frac{x^*y^*(a-a\beta+\alpha\omega)(1-\beta+qm)}{(1+x^*(1-\beta+qm))^2}\Big)\Big(\Big(\frac{r(Ak-2Ax^*-x^{*2})}{k(x^*+A)^2} + \frac{y^*(a-a\beta+\alpha\omega)(1-\beta+qm)}{(1+x^*(1-\beta+qm))^2}\Big)^2 \\ \qquad + \frac{2Ar(A+k)}{k(x^*+A)^2} - \frac{2y^*(a-a\beta+\alpha\omega)(1-\beta+qm)^2}{(1+x^*(1-\beta+qm))^3}\Big) \\ \qquad + \Big(\frac{r(Ak-2Ax^*-x^{*2})}{k(x^*+A)^2} + \frac{y^*(a-a\beta+\alpha\omega)(1-\beta+qm)}{(1+x^*(1-\beta+qm))^2}\Big)\Big(\frac{y^*(a-a\beta+\alpha\omega)(1-\beta+qm)(1-x^*(1-\beta+qm))}{(1+x^*(1-\beta+qm))^2} \\ \qquad + \frac{2A^2rk-2Arkx^*-rx^{*3}-3Arx^{*2}-8A^2rx^*}{k(x^*+A)^3}\Big) \\ \qquad + \frac{8A^2rk-3Arx^{*2}-4A^3r+2Akx^*-4A^2rk}{k(x^*+A)^4} - \frac{y^*(a-a\beta+\alpha\omega)(1-\beta+qm)\Big(1+6x^*(1-\beta+qm)^2(1+x^*(1-\beta+qm))\Big)}{(1+x^*(1-\beta+qm))^5} \\ \qquad - y^*(a-a\beta+\alpha\omega)(1-\beta+qm)^2(1+x^*(1-\beta+qm))^3\Bigg], \end{cases}$$

$$
\begin{cases}
a_{112} = \frac{1}{2}\Bigg[\Bigg(\frac{(a-a\beta+\alpha\omega)(1-\beta+qm)}{(1+x^*(1-\beta+qm))^2} - \frac{ry^*(Ak-2Ax-x^{*2})(a-a\beta+\alpha\omega)}{k(x^*+A)^2(1+x^*(1-\beta+qm))} - \frac{y^{*2}(a-a\beta+\alpha\omega)^2(1-\beta+qm)}{(1+x^*(1-\beta+qm))^3}\Bigg)\Bigg(1 \\
\quad + \frac{rx^*(Ak-2Ax-x^{*2})}{k(x^*+A)^2} \\
\quad + \frac{x^*y^*(a-a\beta+\alpha\omega)(1-\beta+qm)}{(1+x^*(1-\beta+qm))^2}\Bigg) + \frac{rx^*(Ak-2Ax-x^{*2})(a-a\beta+\alpha\omega)(1-\beta+qm)}{k(x^*+A)^2(1+x^*(1-\beta+qm))^2} + \frac{x^*y^*(a-a\beta+\alpha\omega)^2(1-\beta+qm)^2}{(1+x^*(1-\beta+qm))^4} \\
\quad - \frac{y^*(a-a\beta+\alpha\omega)(A^2rk-Arkx^*-rx^{*3}-4A^2rx^*)}{k(x^*+A)^3(1+x^*(1-\beta+qm))} + \frac{(a-a\beta+\alpha\omega)(1-\beta+qm)(1-x^*(1-\beta+qm))}{(1+x^*(1-\beta+qm))^3}\Bigg],
\end{cases}
$$

$$
\begin{cases}
a_{221} = \frac{1}{2}\Bigg[\frac{rx^*(Ak-2Ax-x^{*2})(a-a\beta+\alpha\omega)^2}{k(x^*+A)^2(1+x^*(1-\beta+qm))^2} + \frac{x^*y^*(a-a\beta+\alpha\omega)^3(1-\beta+qm)}{(1+x^*(1-\beta+qm))^4} + \frac{(a-a\beta+\alpha\omega)^2(1-x^*(1-\beta+qm))}{(1+x^*(1-\beta+qm))^3}\Bigg], \\
a_{222} = -\frac{x^*y^*(a-a\beta+\alpha\omega)^3}{6(1+x^*(1-\beta+qm))^3},\ b_{11} = -\frac{\eta y^*(a-a\beta+\alpha\omega)(1-\beta+qm)\Big(2(1+x^*(1-\beta+qm)+\eta(a-a\beta+\alpha\omega)\Big)}{2(1+x^*(1-\beta+qm))^4}, \\
b_{12} = \frac{\eta(a-a\beta+\alpha\omega)}{(1+x^*(1-\beta+qm))^2},\ b_{22} = 0,\ b_{111} = \frac{\eta^2y^*(a-a\beta+\alpha\omega)^2(1-\beta+qm)^2\Big(2(1+x^*(1-\beta+qm))+\eta(a-a\beta+\alpha\omega)\Big)}{3(1+x^*(1-\beta+qm))^7}, \\
b_{112} = -\frac{\eta(a-a\beta+\alpha\omega)(1-\beta+qm)\Big(2(1+x^*(1-\beta+qm))+\eta(a-a\beta+\alpha\omega)\Big)}{2(1+x^*(1-\beta+qm))^4},\ b_{221} = 0,\ b_{222} = 0.
\end{cases}
\tag{4.1}
$$

Funding: The authors extend their appreciation to Prince Sattam bin Abdulaziz University for funding this research work through the project number (PSAU/2026/01/45002)

Data Availability: All data included in this manuscript are available upon request by contacting with the corresponding author.

Conflicts of Interest: The authors declare that there are no conflicts of interest regarding the publication of this paper.

References

[1] A.J. Lotka, Elements of Physical Biology, Williams and Wilkins, Baltimore, 1925.

[2] V. Volterra, Variazioni e Fluttuazioni del Numero d'Individui in Specie Animali Conviventi, Mem. R. Accad. Naz. Lincei Ser. VI 2 (1926), 31–113.

[3] C.S. Holling, The Functional Response of Predators to Prey Density and its Role in Mimicry and Population Regulation, Mem. Entomol. Soc. Can. 97 (1965), 5–60. https://doi.org/10.4039/entm9745fv.

[4] S. Li, X. Wang, X. Li, K. Wu, Relaxation Oscillations for Leslie-Type Predator–Prey Model with Holling Type I Response Functional Function, Appl. Math. Lett. 120 (2021), 107328. https://doi.org/10.1016/j.aml.2021.107328.

[5] M. Lu, J. Huang, Global Analysis in Bazykin's Model with Holling II Functional Response and Predator Competition, J. Differ. Equ. 280 (2021), 99–138. https://doi.org/10.1016/j.jde.2021.01.025.

[6] C.F. Arias, G. Blé, M. Falconi, Dynamics of a Discrete-Time Predator–Prey System with Holling II Functional Response, Qual. Theory Dyn. Syst. 21 (2022), 31. https://doi.org/10.1007/s12346-022-00562-5.

[7] K. Vishwakarma, M. Sen, Influence of Allee Effect in Prey and Hunting Cooperation in Predator with Holling Type-III Functional Response, J. Appl. Math. Comput. 68 (2022), 249–269. https://doi.org/10.1007/s12190-021-01520-1.

[8] Y. Lin, Q. Din, M. Rafaqat, A.A. Elsadany, Y. Zeng, Dynamics and Chaos Control for a Discrete-Time Lotka-Volterra Model, IEEE Access 8 (2020), 126760–126775. https://doi.org/10.1109/access.2020.3008522.

[9] S. Wu, X. Meng, Dynamics of a Delayed Predator-Prey System with Fear Effect, Herd Behavior and Disease in the Susceptible Prey, AIMS Math. 6 (2021), 3654–3685. https://doi.org/10.3934/math.2021218.

[10] S. Wang, L. Niu, On the Global Stability of a Discrete-Time Predator-Prey Model of Kolmogorov Type, Discret. Contin. Dyn. Syst. B 30 (2025), 3526–3540. https://doi.org/10.3934/dcdsb.2025033.

[11] V.S. Sharma, A. Singh, P. Malik, Bifurcation Patterns in a Discrete Predator–Prey Model Incorporating Ratio-Dependent Functional Response and Prey Harvesting, Qual. Theory Dyn. Syst. 23 (2024), 74. https://doi.org/10.1007/s12346-023-00929-2.

[12] S. Yıldız, Ş. Bilazeroğlu, H. Merdan, Stability and Bifurcation Analyses of a Discrete Lotka–Volterra Type Predator–Prey System with Refuge Effect, J. Comput. Appl. Math. 422 (2023), 114910. https://doi.org/10.1016/j.cam.2022.114910.

[13] C. Köme, Y. Yazlik, Stability, Bifurcation Analysis and Chaos Control in a Discrete Predator–Prey System Incorporating Prey Immigration, J. Appl. Math. Comput. 70 (2024), 5213–5247. https://doi.org/10.1007/s12190-024-02230-0.

[14] S.K. Hassan, S.R. Jawad, The Effect of Mutual Interaction and Harvesting on Food Chain Model, Iraqi J. Sci. 63 (2022), 2641–2649. https://doi.org/10.24996/ijs.2022.63.6.29.

[15] O. Francis, T. Aminer, B. Okelo, J. Manyala, Dynamical Analysis of Prey Refuge Effects on the Stability of Holling Type III Four-Species Predator-Prey System, Results Control Optim. 14 (2024), 100390. https://doi.org/10.1016/j.rico.2024.100390.

[16] A.A. Thirthar, S.J. Majeed, K. Shah, T. Abdeljawad, The Dynamics of an Aquatic Ecological Model with Aggregation, Fear and Harvesting Effects, AIMS Math. 7 (2022), 18532–18552. https://doi.org/10.3934/math.20221018.

[17] A.M. Yousef, S.Z. Rida, H.M. Ali, A.S. Zaki, Stability, Co-dimension Two Bifurcations and Chaos Control of a Host-Parasitoid Model with Mutual Interference, Chaos Solitons Fractals 166 (2023), 112923. https://doi.org/10.1016/j.chaos.2022.112923.

[18] Y. Cai, Q. Chen, Z. Teng, G. Zhang, R. Rifhat, Bifurcations in a Discrete-Time Beddington–DeAngelis Prey–Predator Model with Fear Effect, Prey Refuge and Harvesting, Nonlinear Dyn. 113 (2025), 931–969. https://doi.org/10.1007/s11071-024-10232-7.

[19] A.M. Yousef, A.M. Algelany, A.A. Elsadany, Codimension One and Codimension Two Bifurcations in a Discrete Kolmogorov Type Predator–Prey Model, J. Comput. Appl. Math. 428 (2023), 115171. https://doi.org/10.1016/j.cam.2023.115171.

[20] A.A. Elsadany, A.M. Yousef, S.A. Ghazwani, A.S. Zaki, Bifurcation Analysis of a Discrete Basener–Ross Population Model: Exploring Multiple Scenarios, Computation 13 (2025), 11. https://doi.org/10.3390/computation13010011.

[21] A. Almaslokh, A.A. Elsadany, B. Alreshidi, A.S. Zaki, Bifurcation Analysis and Dynamic Behavior of a Discrete Predator–Prey System Incorporating Allee Effects and Environmental Factors, AIMS Math. 11 (2026), 21069–21090. https://doi.org/10.3934/math.2026855.

[22] A.A. Thirthar, P. Panja, S.J. Majeed, K.S. Nisar, Dynamic Interactions in a Two-Species Model of the Mammalian Predator–Prey System: The Influence of Allee Effects, Prey Refuge, Water Resources, and Moonlights, Partial Differ. Equ. Appl. Math. 11 (2024), 100865. https://doi.org/10.1016/j.padiff.2024.100865.

[23] Y.A. Kuznetsov, Elements of Applied Bifurcation Theory, Springer New York, 1998. https://doi.org/10.1007/b98848.

[24] S. Wiggins, Introduction to Applied Nonlinear Dynamical Systems and Chaos, Springer-Verlag, 2003. https://doi.org/10.1007/b97481.

[25] J. Carr, Applications of Centre Manifold Theory, Springer US, 1981. https://doi.org/10.1007/978-1-4612-5929-9.

[26] J. Guckenheimer, P. Holmes, Nonlinear Oscillations, Dynamical Systems, and Bifurcations of Vector Fields, Springer New York, 1983. https://doi.org/10.1007/978-1-4612-1140-2.

[27] C. Robinson, Dynamical Systems: Stability, Symbolic Dynamics, and Chaos, CRC Press, 1998. https://doi.org/10.1201/9781482227871.

[28] D. Hu, X. Liu, K. Li, M. Liu, X. Yu, Codimension-Two Bifurcations of a Simplified Discrete-Time SIR Model with Nonlinear Incidence and Recovery Rates, Mathematics 11 (2023), 4142. https://doi.org/10.3390/math11194142.

[29] V.S. Sharma, S. Mangal, A. Singh, A Complex Dynamics of Discrete-Time Chemostat Model: Codimension-One and Two Bifurcations Analysis, J. Appl. Math. Comput. 71 (2025), 8767–8794. https://doi.org/10.1007/s12190-025-02605-x.

[30] Q. Din, Controlling Chaos and Codimension-Two Bifurcation in a Discrete Fractional-Order Brusselator Model, J. Vib. Control 31 (2025), 2963–2988. https://doi.org/10.1177/10775463241267033.

[31] C. Lei, X. Han, Codimension-Two Bifurcation Analysis of a Discrete Predator–Prey System with Fear Effect and Allee Effect, Nonlinear Anal. Model. Control 30 (2025), 386–404. https://doi.org/10.15388/namc.2025.30.38977.

[32] A.A. Elsadany, A. Almaslokh, S.M. Salman, Codimension Two Bifurcation Analysis of a Discrete Coupled Competition Duopoly Game, Int. J. Anal. Appl. 24 (2026), 12. https://doi.org/10.28924/2291-8639-24-2026-12.

[33] Y.A. Kuznetsov, H.G.E. Meijer, Numerical Bifurcation Analysis of Maps, Cambridge University Press, 2019. https://doi.org/10.1017/9781108585804.